

Article

C–H Bond Activation of Silyl-Substituted Pyridines with Bis(Phenolate)Yttrium Catalysts as a Facile Tool towards Hydroxyl-Terminated Michael-Type Polymers

Thomas M. Pehl [†], Moritz Kränzlein [†], Friederike Adams [†], Andreas Schaffer and Bernhard Rieger ^{*}

WACKER-Chair of Macromolecular Chemistry, Catalysis Research Center, Department of Chemistry, Technical University of Munich, Lichtenbergstr. 4, 85748 Garching near Munich, Germany; thomas.pehl@makro.ch.tum.de (T.M.P.); moritz.kraenzlein@makro.ch.tum.de (M.K.); rike.adams@makro.ch.tum.de (F.A.); andreas.schaffer@makro.ch.tum.de (A.S.)

* Correspondence: rieger@tum.de; Tel.: +49-89-289-13570

† These authors contributed equally to this work.

Received: 8 April 2020; Accepted: 20 April 2020; Published: 22 April 2020



Abstract: Herein, silicon-protected, *ortho*-methylated hydroxy-pyridines were reported as initiators in 2-aminoalkoxy-bis(phenolate)yttrium complexes for rare earth metal-mediated group-transfer polymerization (REM-GTP) of Michael-type monomers. To introduce these initiators, C–H bond activation was performed by reacting $[(\text{ONOO})^{\text{tBu}}\text{Y}(\text{X})(\text{thf})]$ ($\text{X} = \text{CH}_2\text{TMS}$, thf = tetrahydrofuran) with *tert*-butyl-dimethyl-silyl-functionalized α -methylpyridine to obtain the complex $[(\text{ONOO}^{\text{tBu}}\text{Y}(\text{X})(\text{thf})](\text{X} = 4-(4'-(\text{tert}-\text{butyldimethylsilyl})\text{oxy})\text{methyl})\text{phenyl}-2,6\text{-di-methylpyridine}]$. These initiators served as functional end-groups in polymers produced via REM-GTP. In this contribution, homopolymers of 2-vinylpyridine (2VP) and diethyl vinyl phosphonate (DEVP) were produced. Activity studies and end-group analysis via mass spectrometry, size-exclusion chromatography (SEC) and NMR spectroscopy were performed to reveal the initiator efficiency, the catalyst activity towards both monomers as well as the initiation mechanism of this initiator in contrast to commonly used alkyl initiators. In addition, 2D NMR studies were used to further confirm the end-group integrity of the polymers. For all polymers, different deprotection routes were evaluated to obtain hydroxyl-terminated poly(2-vinylpyridine) (P2VP) and poly(diethyl vinyl phosphonate) (PDEVP). Such hydroxyl groups bear the potential to act as anchoring points for small bioactive molecules, for post-polymerization functionalization or as macroinitiators for further polymerizations.

Keywords: rare earth metal-mediated group-transfer polymerization; homogeneous catalysis; C–H bond activation; end-group functionalization; poly(diethyl vinyl phosphonate); poly(2-vinylpyridine); non-metallocenes

1. Introduction

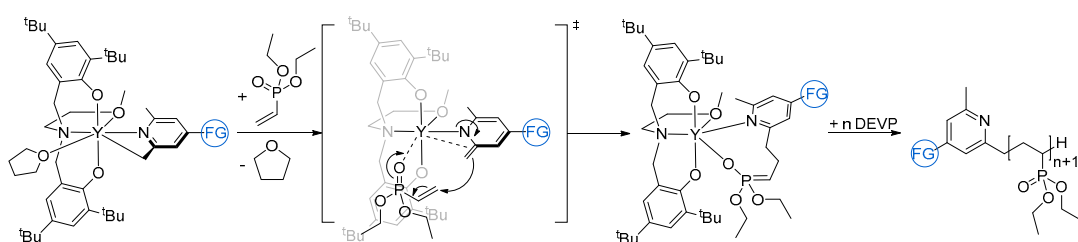
Since the initial discovery of group-transfer polymerization (GTP) of methyl methacrylate (MMA) using silyl ketene acetals by Webster et al. in 1983 [1], this polymerization type has been continuously refined. The application of a neutral samarocene-based complex for the polymerization of MMA by Yasuda et al. in 1992 [2] introduced the field of rare earth metal-based group-transfer polymerization (REM-GTP). Mechanism elucidation on this reaction revealed a repeated 1,4-conjugate addition (Michael-addition) during propagation with a keto-enolate 8-membered cyclic intermediate [1–8]. Since the first polymerization attempts, various organocatalysts, metallocenes and non-metallocenes

were established for the synthesis of highly precise, tailor-made and functional polymers [3,5,7–14]. The scope of available 1,4-Michael-type monomers ranges from differently substituted acrylates, methacrylates, acrylamides or nitrogen bearing monomers (e.g., 2-vinyl pyridine (2VP) to vinyl lactone systems and phosphorous containing monomers, i.e., dialkyl vinyl phosphonates (DAVP) [5,7,15,16].

The broad variety of monomers comes along with individual challenges for each monomer type, such as low activities or initiator efficiencies of the catalysts that have to be solved by the development of catalysts with enhanced performance. These catalysts were able to overcome the obstacles and produced high molecular weight polymers with very narrow molecular weight distributions and were in addition able to induce stereoinformation [10,15,17–21]. This enhanced performance was achieved by e.g., introducing highly sterically demanding ligands to non-metallocenes for stereoregular polymerization of MMA or 2VP [9,10,21], by controlled polymerization of vinyl phosphonates using non-metallocenes, frustrated Lewis pairs or trivalent metallocenes [12,14,15,17,22–24] or by utilizing C–H bond activation to obtain catalysts with higher initiator efficiencies [18]. Further to this, the synthesis of block copolymers was facilitated due to the living character of this polymerization type by simple sequential addition of different monomers with respect to their coordination strength to the metal center [7,25,26]. Additionally, C–H bond activation gave access to post-polymerization functionalization and facilitated the synthesis of new block copolymer structures and polymer architectures [7,18,27–34].

Lanthanide complexes can undergo σ -bond metathesis in a $[2\sigma + 2\sigma]$ cycloaddition which is a very effective method for cleaving C–H bonds in metalorganic chemistry. Trivalent lanthanide and transition metal complexes with a d^0 -configuration do not possess the ability to undergo oxidative addition or reductive elimination, making σ -bond metathesis via C–H bond activation the only possibility of introducing new molecules to this kind of complexes [35–38]. This principle of C–H bond activation was introduced in 1983 by Watson et al. [39,40], showing the activity of Cp^*_2LuX ($X = H, CH_3$) complexes ($Cp^* =$ pentamethylcyclopentadienyl) towards $[2\sigma + 2\sigma]$ cycloaddition with pyridine, benzene or a phosphorylidene. They further discovered the activation of methane in a C–H bond activation reaction with $Cp^*_2LuCH_3$ by ^{13}C isotope labelling. This is the first example of activating the very inert sp^3 -hybridized carbon–hydrogen bonds in methane, which are known to be reluctant to undergo any kind of activation [38–40].

The first example of polymerization catalysts obtained by C–H bond activation was developed by Mashima et al. in 2011 using an yttrium ene-diamido complex for enhancing the initiator efficiencies, but was also used for end-group functionalization of GTP-based polymers as the initiators serve as the end-groups of the polymers (Scheme 1) [18,27,28].

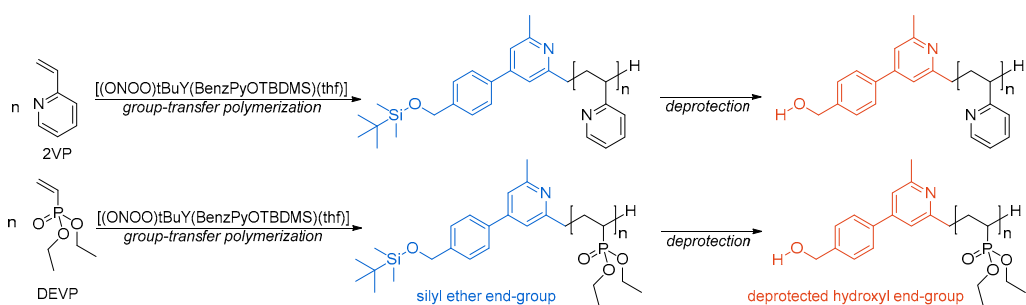


Scheme 1. Synthesis of an end-group functionalized poly(diethyl vinyl phosphonate) (PDEVp) via nucleophilic attack of an α -methylated pyridine initiator of a bis(phenolate)yttrium complex to the first monomer molecule during initiation [9,18,28].

The accessibility to phosphorus- and nitrogen-containing polymers in REM-GTP, especially, poly(diethyl vinyl phosphonate) (PDEVP) with its thermoresponsive behavior and poly(2-vinylpyridine) (P2VP) with its pH-dependent solubility, highlights the potential of this polymerization type to generate smart polymers. After developing capable catalysts using C-H bond activation or catalyst immobilization, differently constituted polymers from vinyl phosphonates and/or 2VP, e.g., block copolymers as drug carriers [29,33], polymer-metal complex conjugates [30],

polymer-biomolecule conjugates [31,32,41] or responsive polymer surfaces were synthesized as smart polymers so far [7,42].

Within this paper, a pathway towards hydroxy-functionalized P2VP and PDEVP is established, since commonly used initiators (e.g., alkyl initiators, cyclopentadienyl) led to solely hydrocarbon-containing end-groups. In this contribution, C–H bond activation is applied as a facile tool towards introduction of hydroxy-groups to Michael-type polymers. Since free hydroxyl groups cannot be introduced to rare earth metals directly due to their high acidity, protection group chemistry was utilized. The complex $[(\text{ONOO})^{\text{tBu}}\text{Y}(\text{CH}_2\text{TMS})(\text{thf})]$ was functionalized with 4-((4'-(*tert*-butyl-dimethylsilyl)oxy)methyl)phenyl)-2,6-dimethylpyridine (BenzPyOTBDMS) in a C–H bond activation reaction to yield the desired catalyst $[(\text{ONOO})^{\text{tBu}}\text{Y}(\text{BenzPyOTBDMS})(\text{thf})]$. This catalyst gave access to P2VP and PDEVP with a silyl ether end-group, which was transformed into a hydroxyl end-group via a deprotection reaction (Scheme 2). Different deprotection reactions of the end-groups were carried out.



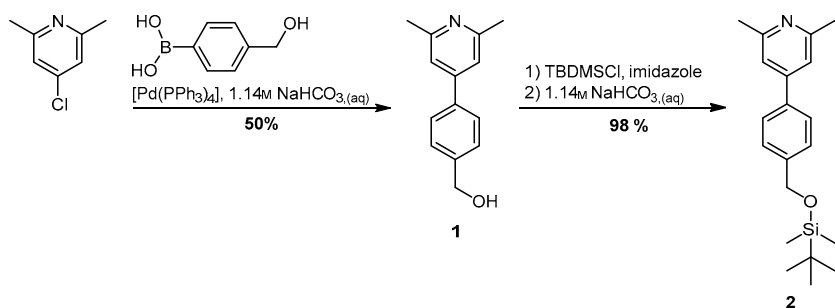
Scheme 2. Synthesis of P2VP (top) and PDEVP (bottom) with hydroxyl end-groups via REM-GTP using the functionalized yttrium catalyst $[(\text{ONOO})^{\text{tBu}}\text{Y}(\text{BenzPyOTBDMS})(\text{thf})]$ and subsequent deprotection.

The hydroxyl end-group was chosen as it could not only be used as a functional group for post-polymerization functionalization (e.g., coupling to biomolecules, fluorescent markers or dyes), but can also act as an anchoring point on surfaces, as a macroinitiator or chain transfer agent for subsequent copolymerization e.g., using immortal ring-opening polymerization [43] enabling the coupling of polyesters with Michael-type polymers. In addition, a commonly used strategy is the application of hydroxy-terminated polymers as precursors for macroinitiators for living-radical polymerizations (ATRP, SET-LRP) facilitating the coupling with non-polar vinyl monomers [44,45].

2. Results and Discussion

2.1. Synthesis of the Functionalized Pyridine 2

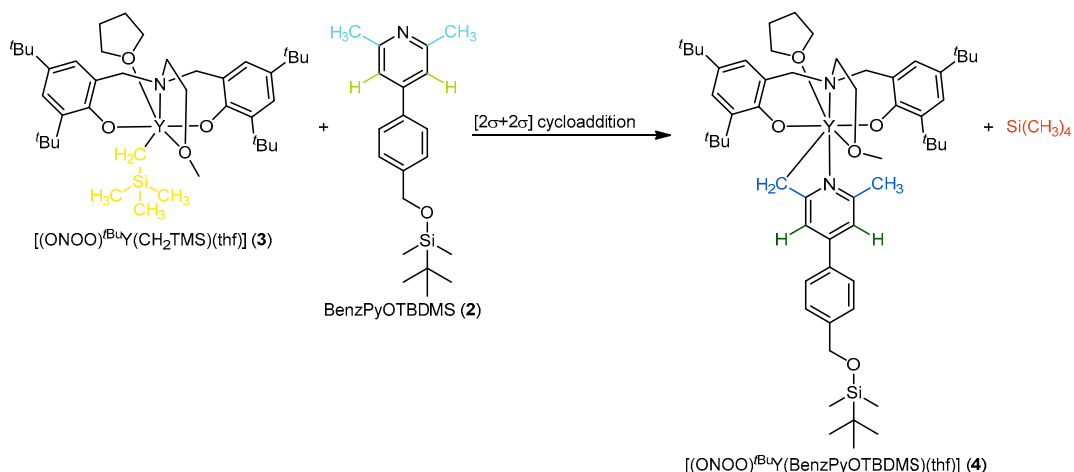
By using purchased 2,6-dimethylpyridine as starting material, 4-chloro-2,6-dimethylpyridine was synthesized according to the literature [32]. Afterwards, Suzuki-coupling was used to react 4-chloro-2,6-dimethylpyridine with 4-hydroxymethyl benzyl boronic acid resulting in the coupling product **1**. To enable C–H bond activation with rare earth metals, acidic protons were masked by protection group chemistry. The hydroxy-group of **1** was converted to a *tert*-butyl-dimethylsilyl protection group (TBDMS) by reaction of **1** with TBDMS-Cl, yielding the protected α -methylated pyridine **2** (Scheme 3). The formation of a trimethyl silyl (TMS) ether instead was not applicable, because hydrogen chloride formed in this reaction cannot be fully quenched, resulting in a pyridinium salt. Using an alkaline work-up, this salt-formation is reversible when using the TBDMS-group instead of the TMS group due to its stability in an aqueous, basic medium [41].



Scheme 3. Synthesis of silyl-protected pyridine 2 starting from 4-chloro-2,6-dimethylpyridine, Suzuki-coupling and subsequent protection.

2.2. C–H Bond Activation of 2 Using 2-Methoxyethylamino-Bis(Phenolate)Yttrium Complex 3

To reveal the general activity of **2** towards C–H bond activation using 2-methoxyethylamino-bis(phenolate)yttrium complex **3** [$(\text{ONO})^{\text{t-Bu}}\text{Y}(\text{CH}_2\text{TMS})(\text{thf})$], the reaction was first monitored in an ^1H -NMR kinetic experiment. **3** can undergo fast and selective C–H bond activation (Scheme 4) with a variety of different methylated pyridines via $[2\sigma + 2\sigma]$ cycloaddition as previously reported [28,30,33].



Scheme 4. σ-Bond metathesis of silyl ether functionalized pyridine **2** and complex **3** to obtain catalyst $[(ONOO)^{t\text{Bu}}Y(\text{BenzPyOTBDMS})(\text{thf})]$ (**4**).

For the ^1H -NMR kinetic investigation on the C–H bond activation, complex **3** and the silyl-protected pyridine **2** were dissolved in deuterated benzene, the mixture was heated to 60 °C and an ^1H -NMR was performed at regular time intervals (Figure 1). As the reaction progresses, the signals of the trimethylsilyl group ($\delta = 0.49$ ppm) and the CH_2 -group ($\delta = -0.40$ ppm) (Figure 1, yellow) of the CH_2TMS -initiator binding to the yttrium center decrease, and simultaneously, a new signal emerged at $\delta = 0.00$ ppm, which corresponded to tetramethyl silane (Figure 1, orange). The signal of the methyl groups in α -position ($\delta = 2.51$ ppm) (Figure 1, light blue) to the nitrogen atom of **2** decreased over time, while two new signals at $\delta = 2.22$ ppm and $\delta = 2.67$ ppm with an integral ratio of 3:2 were measured (Figure 1, dark blue). $[2\sigma + 2\sigma]$ -cycloaddition of one of the methyl groups in α -position of the pyridine with the CH_2TMS group of **3** takes place, resulting in the successful attachment of **2** to the yttrium center. Furthermore, the signal of the two protons adjacent to the methyl groups of **2** ($\delta = 6.97$ ppm, Figure 1, light green) split into two new signals with a ratio of 1:1 at $\delta = 6.25$ ppm and $\delta = 7.07$ ppm (Figure 1, dark green) over the course of the reaction due to an asymmetry caused by coordination to the yttrium-complex. Additionally, the ^1H -NMR kinetic indicates a selective C–H bond activation without the formation of side products.

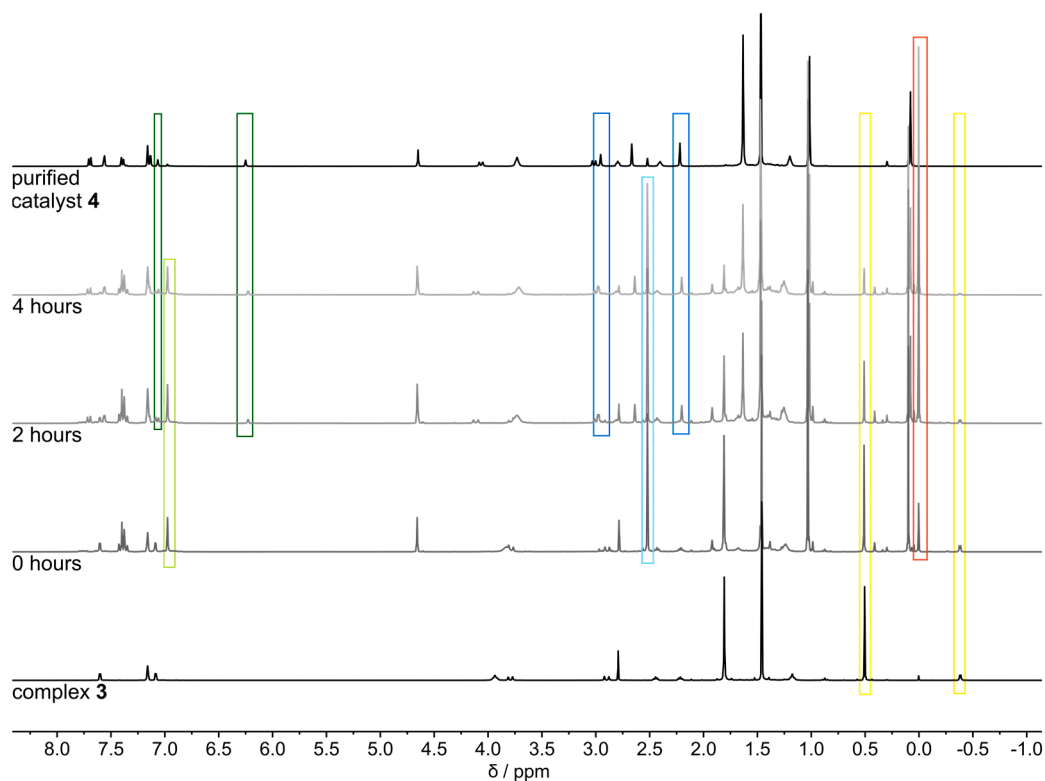


Figure 1. ^1H -NMR kinetic reaction of the σ -bond metathesis of complex **3** with the protected pyridine **2** to obtain silyl-protected catalyst **4** in benzene- d_6 .

As the activation of compound **2** with yttrium-complex **3** on NMR scale was feasible, the catalyst synthesis was scaled up using toluene as the solvent and stirring of the mixture at $60\text{ }^\circ\text{C}$ for 17 h to ensure full conversion. After purification by washing with pentane several times, catalyst **4** could be isolated in 72% yield. The complex was characterized by ^1H -/ ^{13}C -NMR spectroscopy (Figures S1 and S2) and elemental analysis. All methods indicated that despite the highly sterically demanding initiator, tetrahydrofuran is still present in catalyst **4**.

2.3. Investigation on Catalytic Activity of Catalyst **4**

Initially, the catalytic activity of catalyst **4** towards DEVP and 2VP polymerization was investigated. Therefore, the turnover frequency TOF [h^{-1}], initiator efficiency and normalized turnover frequency TOF* [h^{-1}] were determined (Table 1). For determination of the turnover frequency of catalyst **4** towards DEVP, conversions over time were measured via aliquots of a polymerization of DEVP in a catalyst-to-monomer ratio of 1/600 in toluene. Conversions were calculated from ^{31}P -NMR spectra (Figure 2, left) by integration of polymer ($\delta = 30\text{--}31\text{ ppm}$) against monomer ($\delta = 15\text{ ppm}$) signals. After plotting the conversion vs. time, the highest slope of this plot was used for calculating the turnover frequency. For the DEVP polymerization, the turnover frequency is 4320 h^{-1} . Regarding the incomplete initiation shown by an initiator efficiency below 100%, a normalized turnover frequency (TOF*) of 6350 h^{-1} was determined with regards to an initiator efficiency of 68%. Molar masses at the respective conversions were used to reveal the living character of the polymerizations. The living character of the polymerization is confirmed by a linear growth of the molecular weight with increasing conversion of the monomer and narrow polydispersities throughout the whole polymerization (Figure 2, right).

Table 1. Results from kinetic measurements of DEVP and 2VP polymerization with catalyst 4.

Entry	M	[M]/[I] ^a	Conv. ^b (%)	M _{n,calc} ^c (kg mol ⁻¹)	M _{n,abs} ^d (kg mol ⁻¹)	D ^d (-)	I* ^e (%)	TOF (h ⁻¹)	TOF* ^f (h ⁻¹)
1	DEVP	600/1	86	83.1	139	1.29	68	4320	6350
2	2VP	400/1	99	40.8	55.7	1.02	67	500	750

^a Monomer-to-catalyst ratio, $c_{\text{Cat},0} = 2.3 \text{ mmol/mL}$, toluene, 25°C ; ^b Conversion calculated via aliquot method; ¹H-NMR (2VP) or ³¹P-NMR (DEVP) spectra, ^c $M_{n,\text{calc}}$ from $M_{n,\text{calc}} = M \times ([M]/[\text{Cat}]) \times \text{conversion}$ ^d Determined via SEC (P2VP: DMF+LiBr, 30°C , $\text{dn}/\text{dc} = 0.149 \text{ mL g}^{-1}$ with triple detection SEC; PDEVP: THF:H₂O = 1:1, 40°C , $\text{dn}/\text{dc} = 0.0922 \text{ mL g}^{-1}$, SEC-MALS), polydispersity calculated from $M_{w,\text{abs}}/M_{n,\text{abs}}$ ^e Initiator efficiency I^* at the highest slope in time-conversion plot via $I^* = M_{n,\text{calc}}/M_{n,\text{abs}}$; ^f normalized TOF using I^* ; $\text{TOF}^* = \text{TOF}/I^*$.

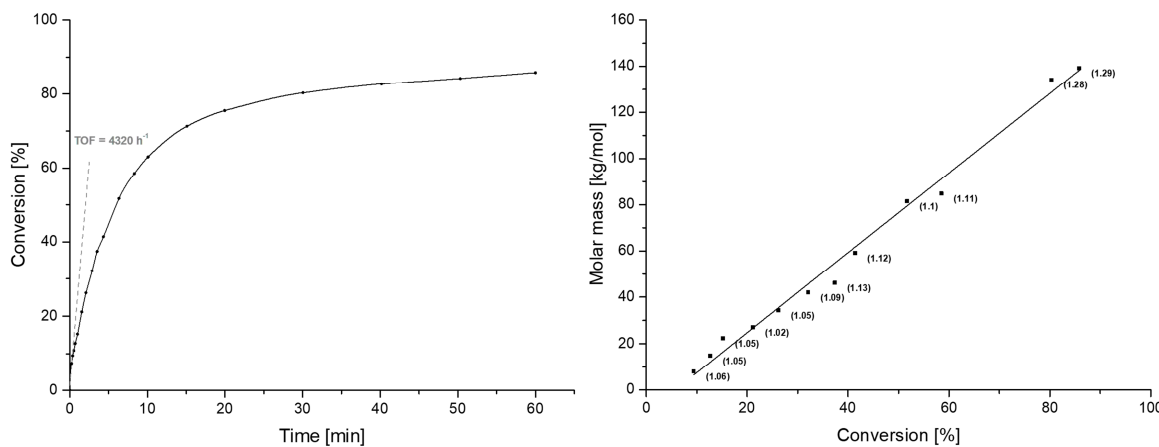


Figure 2. Time-conversion plot (left) and conversion-molar mass plot (right) of the DEVP polymerization with catalyst **4**.

The turnover frequency of catalyst **4** for 2VP polymerization was determined by performing a polymerization with a monomer-to-catalyst ratio of 400/1 in toluene at room temperature. Aliquots were taken from the reaction mixture at regular time intervals and conversions were calculated from $^1\text{H-NMR}$ via conversion = $(I_{\text{Pol+Mon}} (\delta = 7.9\text{--}8.6 \text{ ppm}) - I_{\text{Mon}} (\delta = 5.4 \text{ ppm})) / I_{\text{Pol+Mon}}$ ($\delta = 7.9\text{--}8.6 \text{ ppm}$) (Figure 3, left). A turnover frequency of 500 h^{-1} and a normalized turn over frequency of 750 h^{-1} were calculated. For 2VP polymerization, the living character was confirmed with the conversion–molar mass plot (Figure 3, right).

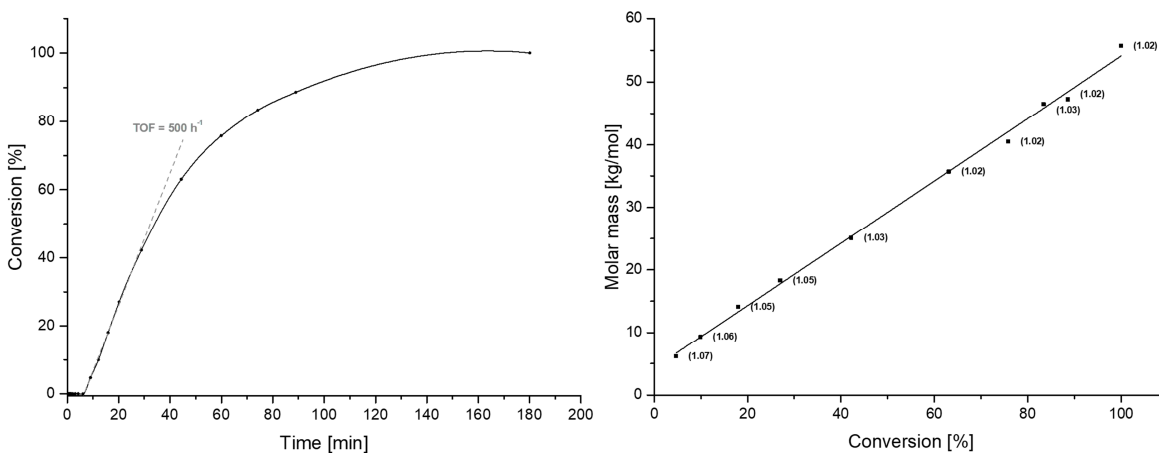


Figure 3. Time–conversion plot (left) and conversion–molar mass plot (right) of 2VP polymerization with catalyst **4** (Table 1, entry 2).

Because the initiator is not involved in the propagation step, the initiator has no influence on the catalyst activity, which is only determined by the metal center and the steric hinderance of the ligand. Catalyst **4** should therefore have a similar normalized turn over frequency as bis(phenolate)yttrium catalysts bearing the same ligand system such as complex **3** or a structure analogue bis(phenolate)yttrium complex such as $[(\text{ONO})^t\text{BuY}(\text{sym-col})(\text{thf})]$ (*sym-col* = 2,4,6-trimethylpyridine), which only differs in the initiator [9,28].

For DEVP, the polymerization proceeds without an initiation delay in the expected fashion, however, the turnover frequency of 4320 h^{-1} is about one magnitude higher than reported in the literature for complex **3**, indicating a different polymerization mechanism [19]. For 2VP, the normalized turnover frequency of 750 h^{-1} is in the same range as reported in the literature for complexes with the same ligand system [19,28,30], but in the time–conversion plot, an initiation delay of about 5 min was observed. This is in contradiction to the behavior of the other C–H bond activated catalysts reported in literature, which do not show initiation periods [28]. We suggest that catalyst **4** may not be present in the assumed monometallic state, but rather in a bimetallic state, since bimetallic complexes showed initiation periods in 2VP polymerization [9]. The dimerization might cause a detachment of the aminomethoxy handle from the metal center and the silyl ether group could be coordinating the yttrium instead. Due to a different chemical structure of the ligand after dissociation into a monomolecular species, the turnover frequency for DEVP could be higher than those reported [19]. As the coordination strength of 2VP is weaker than the one of DEVP [7,28], the dissociation period might be longer for 2VP resulting in an initiation delay. Despite this behavior, catalyst **4** polymerized DEVP and 2VP in a highly controlled way under mild conditions with very low polydispersities. In comparison, 2VP polymerization seems to be more controlled than DEVP polymerization, because the polydispersity of PDEVP increased over the course of the reaction, most likely due to undesired side reactions.

2.4. Polymerization Results

2.4.1. End-Group Analysis of PDEVP and P2VP Produced with Catalyst **4**

For obtaining highly defined, hydroxyl-terminated Michael-type polymers, a quantitative attachment of initiator **2** as an end-group is the main prerequisite. Therefore, a detailed end-group analysis of PDEVP and P2VP was performed via NMR spectroscopy, mass spectrometry and SEC to validate the attachment of initiator **2** to the polymer chains.

An ESI-MS of oligomeric DEVP (Figure 4) was recorded after reacting catalyst **4** with DEVP in a 1:6 ratio in toluene, quenching the polymerization with ethanol after 5 min and by immediate measurement of the reaction mixture in acetonitrile. The initiating pyridine **2** attached to the oligomer was observed in the ESI-MS spectrum by a mass shift of 327 m/z (mass of initiator **2** minus one proton) of the DEVP oligomers ($\text{m/z} = ((M_{\text{Ini}} - \text{H}) + n \times M_{\text{DEVP}} + \text{H} + \text{H})^+$, $n = 2-5$), while unreacted pyridine **2** ($\text{m/z} = 328.5$) and ligand ($\text{m/z} = 512.9$) were observed as well. Since the initiating groups were clearly visible in the ESI-MS, a nucleophilic transfer reaction of the initiator via a monomer insertion into an yttrium carbon bond during the initiation is evident, leading to the desired end-group (Scheme 1). Due to the exclusive presence of signals corresponding to nucleophilic transfer reaction, an initiation via deprotonation is excluded [15,19,30].

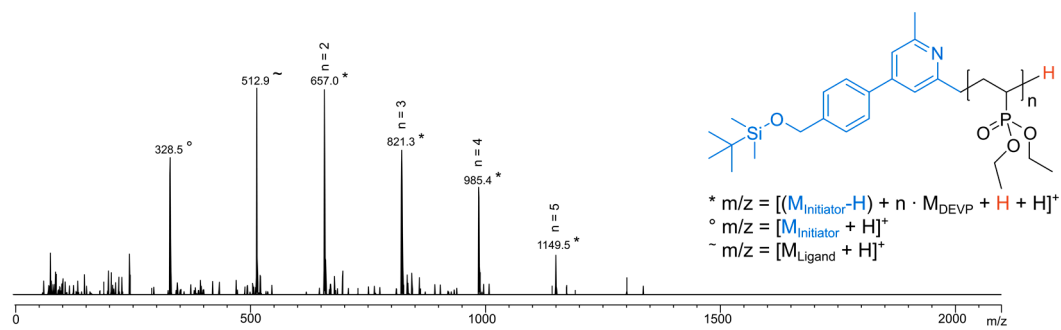


Figure 4. End-group analysis via ESI-MS of oligomeric DEVP ($n = 2\text{--}5$) produced with catalyst 4 ($[4]/[\text{DEVP}] = 1:6$, 25°C , 10 min, toluene) in acetonitrile.

For P2VP, a MALDI-MS spectrum was recorded of purified 2VP oligomers from a reaction of catalyst 4 with 24 equivalents of 2VP in toluene (Figure 5). In this spectrum, a series of signals corresponding to $\text{m/z} = [(\text{M}_{\text{Initiator}} - \text{H}) + n \times \text{M}_{\text{2VP}} + \text{H} + \text{H}]^+$ with $n = 7\text{--}37$ were observed, representing the 2VP oligomers functionalized with the protected initiator 2. This not only underlines a covalently bonded initiator to the polymer chain, but also further substantiates the assumed initiation mechanism of a nucleophilic attack of the methyl pyridine 2 to the first monomer unit [19,30].

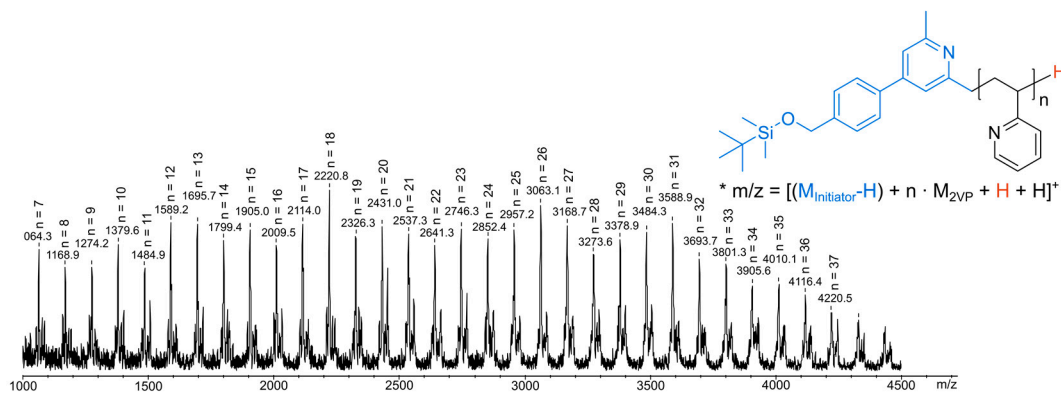


Figure 5. End-group analysis of oligomeric 2VP ($n = 7\text{--}37$) produced with catalyst 4 ($[4]/[2\text{VP}] = 1:24$, 25°C , 3 h, toluene) via MALDI-MS in a dithranol matrix and sodium trifluoroacetate as matrix additive.

As free initiator or unfunctionalized polymers would disturb a successful post-polymerization functionalization, diffusion ordered spectroscopy (DOSY) was applied. To check whether the unbonded initiator is still present in the purified polymers, a DOSY of PDEVP with a number-average molecular weight of about 45 kg mol^{-1} was recorded (Figure S3). In this spectrum, the signals assigned to the methyl groups ($\delta = 0.10 \text{ ppm}$) and the *tert*-butyl group ($\delta = 0.94 \text{ ppm}$) of the silyl protection group of the initiator can be observed at the same diffusion coefficient as the polymer signals, indicating that no free initiator 2 is present in the PDEVP polymer. Analogously, a DOSY spectrum of purified P2VP with a number-average molecular weight of about 35 kg mol^{-1} (Figure S4) is recorded to check for the free initiator in the polymer sample. The silyl signals of the TBDMS-group at $\delta = 0.11 \text{ ppm}$ (methyl silyl) and $\delta = 0.95 \text{ ppm}$ (*tert*-butyl silyl) appear at the same diffusion coefficient as the polymer. Combining the results from mass spectrometry and DOSY-NMR measurement, a functionalization of the polymers with initiator 2, without free initiator remaining in the polymer samples, can be confirmed.

2.4.2. Polymerization of DEVP and 2VP with Catalyst 4

Catalyst 4 was further studied in homopolymerizations of DEVP and 2VP to evaluate the influence of the solvent and the monomer-to-catalyst ratio on the molar masses and polydispersities of the obtained polymers and the initiator efficiency of 4, as these are critical parameters for obtaining highly defined

polymers with a high end-group integrity. As similar heteroaromatic bis(phenolate)yttrium catalysts are well-known to polymerize 2VP and DEVP rapidly at room temperature, higher temperatures were not used in this study [28]. In Table 2, the homopolymerization results of DEVP are summarized.

Table 2. Results of the REM-GTP of DEVP with catalyst 4.

Entry	[DEVP]/[4] ^a	Solvent ^b	Conv. ^c (%)	M _{n,calc} ^d (kg mol ⁻¹)	M _{n,abs} ^e (kg mol ⁻¹)	M _{n,NMR} ^f (kg mol ⁻¹)	D ^e (-)	I ^g (%)
1	200/1	toluene	99	31.8	34.6	42.3	1.07	92
2	200/1	thf	99	32.8	38.0	48.3	1.13	86
3	200/1	dcm	44	14.8	25.0	34.0	1.29	59
4	100/1	toluene	99	15.8	16.6	22.5	1.04	95
5	400/1	toluene	96	61.8	104	122.3	1.33	58

^a Monomer-to-catalyst ratio, n_{Cat} = 13.5 mmol; ^b Reaction time 60 min at 25 °C, 2 mL of solvent; ^c Calculated from ³¹P-NMR spectrum of aliquots at the end of the reaction via ratio of signals of the polymer (δ = 30–31 ppm) and the monomer (δ = 15 ppm); ^d M_{n,calc} from M_{n,calc} = M × (([M]/[Cat]) × conversion); ^e Determined via SEC-MALS in 50:50 THF/H₂O = 1:1, 40 °C, dn/dc = 0.0922 mL g⁻¹, polydispersity calculated from M_{w,abs}/M_{n,abs}; ^f calculated from ¹H-NMR M_{n,NMR} = (I_{Et}/4) M_{DEVP} + M_{Initi}; ^g I = M_{n,calc}/M_{n,abs} at the end of the reaction.

As the kinetic measurement of DEVP with catalyst 4 has shown, the initiator efficiency was reduced when using a high monomer-to-catalyst ratio. Therefore, lower monomer-to-catalyst ratios of 100/1 to 400/1 were used in batch reactions, as these polymerizations proceeded too fast for kinetic measurements. Different solvents were chosen to study their influence of different solvents on the initiator efficiency and activity of 4. For both toluene and tetrahydrofuran, full conversion was reached within the reaction time of 60 min. These polymers had a very narrow molecular weight distribution and initiator efficiencies were high (86–92%) when using a monomer-to-catalyst ratio of 100/1 or 200/1. The polymerization in dichloromethane proceeded much slower, with only 44% conversion after 60 min, broader polydispersity of the polymers and lower initiator efficiency of 4. When the monomer-to-catalyst ratio for the polymerization in toluene as the most suiting solvent is increased, the polydispersity increased while the initiator efficiency decreased. The decreased initiator efficiency was most likely attributed to impurities, deactivating the catalyst species when the monomer loading was too high. Comparing the initiator efficiencies of catalyst 4 (86–92%) for 1/200 catalyst–monomer ratios to the initiator efficiency of the non-C–H bond activated complex 3 (36%) [28], I is significantly increased. This is due to a suppression of deprotonation as the initiation pathway for DEVP by C–H bond activation on such bis(phenolate)yttrium catalysts. The initiator efficiency of [(ONOO)^{tBu}Y(sym-col)(thf)] of I = 73% [28] is also slightly lower than those of catalyst 4 despite the high steric demand of 4. The polydispersities of PDEVP prepared with catalyst 4 were in the same range as those reported in the literature ($D = 1.02\text{--}1.10$) [18,28].

Additionally, the incorporation of the TBDMS-functionalized pyridine 2 in the polymers facilitates a reliable calculation of the number-average molecular weight from ¹H-NMR spectroscopy via the silyl ether end-group, and allowed a comparison with the number-average molecular weight obtained from absolute size-exclusion chromatography (SEC). For PDEVP, the molecular weights from ¹H-NMR spectra (Figure S5) were calculated by normalization of the silyl methyl signals (δ = 0.10 ppm, I_{Me(TBDMS)} = 6) of the TBDMS-group to 6 and calculation of the molar mass with using the integral of the methylene unit in the ethyl groups on the PDEVP side chain (δ = 4.11 ppm, I_{Et}, 4 protons per repeating unit). The signals corresponding to the methyl groups of the PDEVP side chains and to the *tert*-butyl group in the initiator have shown to be unsuited due to overlapping with other signals in some polymer samples. The molecular weight was then calculated as M_{n,NMR} = (I_{Et}/4) M_{DEVP} + M_{Initi}, assuming a quantitative incorporation of the initiator as proved by ESI-MS and DOSY measurements. The absolute molar mass is determined using SEC-MALS (Figure S7). The low deviation between the number-average molar masses obtained from SEC and calculated from ¹H-NMR (1%–24%) underline again a quantitative incorporation of the initiator. The deviations all show the same trend of overestimating the molecular weights from ¹H-NMR compared to those determined via SEC-MALS.

The polymerization behavior of catalyst **4** towards 2VP was investigated with regard to the same parameters as tested for DEVP polymerization (Table 3).

Table 3. Results of the REM-GTP of 2VP with catalyst **4**.

Entry	[2VP]/[4] ^a	Solvent ^b	Conv. ^c (%)	M _{n,calc} ^d (kg mol ⁻¹)	M _{n,abs} ^e (kg mol ⁻¹)	M _{n,NMR} ^f (kg mol ⁻¹)	D ^e (-)	I ^g (%)
1	200/1	toluene	99	22.1	25.0	27.2	1.04	89
2	200/1	thf	22	5.3	21.5	21.5	1.31	25
3	200/1	dcm	99	19.0	22.6	26.9	1.06	84
4	100/1	toluene	99	10.5	12.8	11.1	1.09	82
5	400/1	toluene	98	42.2	58.4	58.8	1.01	72

^a Monomer-to-catalyst ratio, n_{Cat} = 13.5 mmol; ^b Reaction time 60 min at 25 °C, 2 mL of solvent; ^c Calculated from ¹H-NMR of aliquots via conversion = (I_{Poly+Mon} (δ = 7.9–8.6 ppm) – I_{Mon} (δ = 5.4 ppm)) / I_{Poly+Mon} (δ = 7.9–8.6 ppm); ^d M_{n,calc} from M_{n,calc} = M × ([M]/[Cat]) × conversion ^e Determined via SEC in DMF+LiBr (30 °C, dn/dc = 0.149 mL g⁻¹) with triple detection, polydispersity calculated from M_{w,abs}/M_{n,abs}; ^f calculated from ¹H-NMR as M_{n,NMR} = I_{Ar} × M_{2VP} + M_{Ini}; ^g I = M_{n,calc}/M_{n,abs} at the end of the reaction.

Toluene and dichloromethane were appropriate solvents for the synthesis of P2VP, as polymerizations in both solvents reached full conversion within 60 min while maintaining narrow polydispersities and high initiator efficiencies (I = 72–89%) at all monomer-to-catalyst ratios. The polymerization of 2VP in tetrahydrofuran proceeds much slower, with only 22% conversion after 60 min, while leading to broader polydispersities of the polymers. In addition, catalyst **4** only showed a low initiator efficiency (25%). This behavior is attributed to the weak coordination strength [6,28] of 2VP to the yttrium center and a competitive coordination of 2VP and tetrahydrofuran leads to an initiation delay, broadening of the polydispersity, lowering of the initiator efficiency and enhancing potential side reactions. Since DEVP is known to have a higher coordination strength to rare earth metal complexes, this phenomenon was not observed during DEVP polymerization. In general, tetrahydrofuran can be considered a well-suited solvent for REM-GTP as long as the coordination strength of the monomer to the metal center is stronger in comparison to the coordination strength of THF. Additionally, the tacticity of the P2VP was determined using ¹³C-NMR according to the literature (Figure S9). As expected for this metal center and ligand, atactic P2VP was obtained, since the initiator did not influence the tacticity [9]. Comparing the initiator efficiencies of 72–89% of complex **4** to those reported in the literature (complex **3**: I = 99% [9,28]; [(ONO)^tBuY(sym-col)(thf)]: I = 42% [28]), the initiator efficiency of complex **4** is slightly decreased compared to **3** but is considerably higher than those reported for the C–H bonded analogue. This decrease in I of **4** compared to **3** for 2VP can be attributed to an electronic overload on the yttrium center, however, the initiator efficiency using the new initiator **2** is still increased compared to sym-collidine as initiator [30]. As for PDEVP, the polydispersities of P2VP synthesized with catalyst **4** matched with values reported in the literature [9,28,30].

Regarding the molecular weight calculation using ¹H-NMR spectroscopy, the calculation was performed using the integral of the protons in α -position of the nitrogen atom in the aromatic ring (δ = 8.0–8.6 ppm, I_{Ar}, one proton per repeating unit) (Figure S8), giving M_{n,NMR} = I_{Ar} × M_{2VP} + M_{Ini}, which was compared to the absolute number-average molecular weight determined from SEC using triple detection (Figure S10). The signals of the *tert*-butyl group as well as other aromatic signals from P2VP have shown to be unsuited for calculation due to signal overlapping issues. Molecular weights determined via ¹H-NMR and SEC deviate only by 0–16% and are in quite good agreement, again indicating full end-group functionalization.

Overall, highly defined PDEVP and P2VP with tunable molecular weights and narrow polydispersities under mild conditions were synthesized using catalyst **4**. For different catalyst-monomer ratios in suiting solvents, a high end-group integrity was achieved. The combination of NMR analytics, mass spectroscopy, DOSY and SEC confirmed a quantitative end-group functionalization.

2.5. Deprotection of PDEVP and P2VP

To recover the free hydroxyl group from the silyl ether protected polymer, different deprotection strategies (A/B/C) were tested for PDEVP and P2VP (Scheme 5) [46–49]. $^1\text{H-NMR}$ spectra of the polymers were used to evaluate the degree of the silyl group removal upon deprotection. With regards to possible side reactions at the pendant groups or chain cleavage, SEC and NMR spectroscopy were used to check the structural integrity of the polymer after the deprotection reaction.



Scheme 5. Removal of the TBDMS protection group of PDEVP and P2VP using different reaction conditions (A/B/C).

As a first approach (A), deprotection using tetra-*n*-butyl ammonium fluoride (TBAF) as an anhydrous fluorine source in dry tetrahydrofuran was tested. An excess of 50 equiv. TBAF was used for the deprotection of PDEVP and P2VP. The reaction was stirred under ambient conditions overnight and purified with an aqueous work-up. While this reaction ensured a quantitative cleavage of the TBDMS ether for PDEVP with no side reactions or chain-breakage, it was not applicable for P2VP, because polymer deprotection was incomplete and side reactions were detected by $^1\text{H-NMR}$ spectroscopy. In a second approach, deprotection strategy B, an acid-based deprotection with $\text{HCl}_{(\text{aq})}$ in ethanol under ambient conditions, was performed, which gave fully deprotected P2VP after a basic work-up. No alteration of the P2VP chain itself was verified using NMR spectroscopy and SEC (Figure S11 and S12). However, this reaction leads to the formation of side products for PDEVP, which were insoluble in dioxane, indicating side-reactions such as saponification to the free phosphonic acid or crosslinking between polymer chains. To obtain a method suitable for both polymers, and able to also deprotect block copolymers consisting of both subunits, strategy C was tested. This method involved the treatment of the polymers with glacial acetic acid in a tetrahydrofuran-water mixture under ambient conditions. Both polymer types, PDEVP (Figures S13 and S14) and P2VP, were deprotected completely within 24 h without the occurrence of side reactions or polymer degradation. Using this reaction, hydroxyl-terminated PDEVP and P2VP were synthesized. All polymers were analyzed using $^1\text{H-NMR}$ and SEC (Table 4).

Table 4. Results from SEC before and after deprotection of PDEVP and P2VP with the different reactions A/B/C.

Entry	Polymer	Deprotection Procedure	Before Deprotection		After Deprotection	
			$M_{n,\text{abs}}^a$ (kg mol^{-1})	D^a (-)	$M_{n,\text{abs}}^a$ (kg mol^{-1})	D^a (-)
1	PDEVP	A	43.4	1.11	40.6	1.18
2	P2VP	B	25.2	1.05	29.0	1.05
3	PDEVP	C	38.0	1.13	34.3	1.11
4	P2VP	C	25.8	1.09	28.7	1.10

^a Determined via SEC-MALS (PDEVP) or SEC using triple detection (P2VP).

3. Materials and Methods

3.1. Materials

All air and moisture sensitive compounds were prepared using Standard Schlenk techniques in dried glass flasks, using argon as inert gas or handled in an argon-filled glove box. Chemicals were purchased from Sigma-Aldrich (St. Louis, MI, USA), ABCR (Karlsruhe, Baden-Wuerttemberg,

Germany) or TCI Chemicals (Tokyo, Japan) and were used without further purification unless stated otherwise. Diethyl vinyl phosphonate and 2-vinylpyridine were stirred at room temperature over CaH_2 and distilled prior to use. Dry solvents were obtained from a MBraun MB-SPS-800 (Garching-Hochbrück, Bavaria, Germany) solvent purification system by drying over activated alumina, and were stored on 3 Å molecular sieve. DEVP, the $(\text{ONOO})^{\text{tBu}}$ -ligand, 2,6-dimethylpyridine-N-oxide, 4-chloro-2,6-di-methylpyridine, LiCH_2TMS , $\text{Y}(\text{CH}_2\text{TMS})(\text{thf})_2$ and $[(\text{ONOO})^{\text{tBu}}\text{Y}(\text{CH}_2\text{TMS})(\text{thf})]$ were synthesized according to the literature [19,32,50–52].

3.2. Instrumentalization

Nuclear magnetic resonance spectroscopy (NMR) was performed at room temperature on either a Bruker Ascend spectrometer (Billerica, MA, USA) or a Bruker AV500C cryo-NMR spectrometer (Billerica, MA, USA) as indicated (^1H -NMR: 400 MHz/500 MHz; ^{13}C -NMR: 125 MHz; ^{29}Si -NMR: 80 MHz; ^{31}P -NMR: 162 MHz). All ^1H -NMR spectra were referenced to the residual proton signal of the deuterated solvent, ^{13}C -NMR spectra were referenced to the carbon signal of the deuterated solvent, background correction and phase correction were performed using MestreNova. Diffusion-ordered spectroscopy (DOSY) was measured on a Bruker AV-HD400 (Billerica, MA, USA) with 16 scans at room temperature and was transformed using the Bayesian method with a resolution factor of 5 using MestreNova. Signal multiplicities were abbreviated as following: s—singlet, d—duplet, t—triplet, m—multiplet.

Average absolute molecular weights and polydispersities of the polymers were determined via size-exclusion chromatography (SEC) with a sample concentration of 2 mg mL^{-1} . Measurements of PDEVP were performed using size-exclusion chromatography coupled with multi-angle light scattering (SEC-MALS), with $\text{THF:H}_2\text{O} = 1:1$ (with 9 g/L *tetra*-butyl-ammonium bromide and 272 mg L^{-1} 2,6-di-*tert*-butyl-4-methylphenol) as eluent at 40°C , equipped with two Agilent PolarGel M columns (Santa Clara, CA, USA). For detection, a Wyatt Dawn Heleos II MALS light scattering unit (Santa Barbara, CA, USA) and a Wyatt Optilab rEX 536 RI unit (Santa Barbara, CA, USA) were used, the absolute molecular weight was determined using an experimentally measured $\text{dn/dc} = 0.0922 \text{ mL g}^{-1}$. Measurements of P2VP were performed on an Agilent PL-GPC 50 (Santa Clara, CA, USA) with an integrated RI unit, two light scattering detectors (15° and 90°) and a differential pressure viscosimeter with two Agilent PolarGel M columns. As eluent *N,N*-dimethylformamide (with 2.096 g/L lithium bromide added) at 30°C was used, absolute molecular weights were determined using $\text{dn/dc} = 0.149 \text{ mL g}^{-1}$ from the literature [30].

Electron-spray ionization mass spectrometry (ESI-MS) measurements of DEVP oligomer samples (catalyst-to-monomer ratio = 1:6, reaction time 5 min in toluene, quenched with ethanol) were performed on a Varian 500-MS (Palo Alto, CA, USA) with MeCN as the solvent in positive ionization mode (70 eV). Recorded mass spectra were analyzed using MS Data Review.

Matrix-assisted laser desorption ionization mass spectrometry (MALDI-MS) was performed on a Bruker Daltonics ultraflex TOF/TOF (Billerica, MA, USA). Oligomer samples of 2VP with a concentration of 2 mg mL^{-1} in THF were prepared and 3 μL of this solution was mixed with 1 μL of matrix solution (saturated dithranol in H_2O (+ 0.1 vol % TFA):MeCN = 2:1) and 1 μL of 5 mg mL^{-1} sodium trifluoroacetate in H_2O (+ 0.1 vol % TFA):MeCN = 2:1. The mass spectra were recorded in linear positive mode without deflection and gating. Spectra interpretation was performed using Bruker FlexAnalysis.

Lyophilization was performed on a VaCo 5-II-D from Zirbus technology GmbH (Bad Grund, Lower Saxony, Germany), with a pressure of 2 mbar and a condenser temperature of -90°C . PDEVP was dissolved in either water or 1,4-dioxane, P2VP is dissolved in either benzene or 1,4-dioxane prior to freezing in liquid nitrogen.

Elemental analysis was performed by the Laboratory for Microanalytics at the Institute of Inorganic Chemistry at the Technical University of Munich, Department of Chemistry, Catalysis Research Center.

3.3. Synthesis of Catalyst 4 [(ONOO)^{tBu}Y(BenzPyOTBDMS)(thf)]

In total, 2.77 g (3.33 mmol, 1.0 equiv.) of complex **3** (ONOO^{tBu})Y(CH₂TMS)(thf) were dissolved in 30 mL dry toluene and 1.09 g (3.66 mmol, 1.1 equiv.) of the protected pyridine **2** dissolved in 6 mL dry toluene were added. The reaction mixture was stirred at 60 °C for 17 h before the solvent was removed in vacuo leaving a red, oily solid. Upon addition of 2 × 20 mL dry pentane and subsequent removal of the solvent in vacuo, a yellow precipitate was formed, which is subsequently washed with 2 × 25 mL dry pentane before drying under vacuum. Catalyst **4** [(ONOO)^{tBu}Y(BenzPyOTBDMS)(thf)] is obtained as yellow solid (2.57 g, 2.63 mmol, 72%).

¹H-NMR (400 MHz, C₆D₆, 300 K): δ (ppm) = 0.08 (s, 6H, Si(CH₃)₂), 1.02 (s, 9H, SiC(CH₃)₃), 1.16–1.22 (m, 4H, CH₂,thf), 1.47 (s, 18H, ^tBu_{ligand}), 1.63 (s, 18H, ^tBu_{ligand}), 2.21 (s, 3H, CH₃,pyridine), 2.41 (t, ³J_{H,H} = 4.8 Hz, 2H, NCH₂CH₂OMe), 2.66 (s, 3H, OCH₃), 2.80 (t, ³J_{H,H} = 4.8 Hz, 2H, NCH₂CH₂OMe), 2.96 (s, 2H, YCH₂,pyridine), 3.01 (d, ²J_{H,H} = 12.5 Hz, 2H, ArCH₂,ligand), 3.73–3.77 (m, 4H, OCH₂,thf), 4.07 (d, ²J_{H,H} = 12.5 Hz, 2H, ArCH₂,ligand), 4.65 (s, 2H, CH₂OSiR₃), 6.24 (s, 1H, H_{Ar,pyridine}), 7.06 (s, 1H, H_{Ar,pyridine}), 7.13 (d, ⁴J_{H,H} = 2.6 Hz, 2H, H_{Ar,ligand}), 7.39 (d, ³J_{H,H} = 8.0 Hz, 2H, H_{Ar,benzyl}), 7.56 (d, ⁴J_{H,H} = 2.6 Hz, 2H, H_{Ar,ligand}), 7.70 (d, ³J_{H,H} = 8.2 Hz, 2H, H_{Ar,benzyl}).

¹³C-NMR (125 MHz, C₆D₆, 300 K): δ (ppm) = 5.1, 18.6, 23.7, 25.2, 26.2, 30.3, 32.3, 34.3, 49.5, 54.5, 59.7, 65.1, 65.2, 70.9, 72.9, 105.8, 113.9, 124.2, 124.5, 125.8, 126.8, 127.0, 136.6, 136.8, 139.6, 141.7, 147.3, 156.8, 161.7 (d, ¹J_{Y,C} = 2.5 Hz), 167.4.

²⁹Si-NMR (80 MHz, C₆D₆, 300 K): δ (ppm) = 19.7.

EA: Calc: C 68.65, H 8.79, N 2.81, O 8.02, Si 2.82, Y 8.91. Found: C 68.53, H 9.12, N 2.81.

For the ¹H-NMR kinetic experiment, 10 mg (0.013 mmol, 1 equiv.) of complex **3** were dissolved in 0.4 mL deuterated benzene and 6.88 mg (0.021 mmol, 1.6 equiv.) protected pyridine **2** were dissolved in 0.1 mL deuterated benzene. Both solutions were mixed inside a Young NMR tube and the reaction mixture was heated to 60 °C. Every 30 min, a proton-NMR spectrum was measured to evaluate the reaction progress.

3.4. Polymerization Procedure

For the polymerization of DEVP or 2VP, 13.5 mg (13.5 μmol, 1.0 equiv.) of catalyst **4** were weighed into a dried screw cap vial and dissolved in 2 mL dry solvent (toluene, thf or dichloromethane). Under vigorous stirring the calculated amount of monomer (50 equiv., 100 equiv., 200 equiv., 400 equiv. or 600 equiv.) was added in one portion and the reaction was stirred at 25 °C for 60 min. An aliquot of 0.1 mL of the reaction mixture was taken and quenched in wet CDCl₃ (PDEVP) or MeOD (P2VP) before stopping the reaction with 0.5 mL methanol. The polymers were precipitated in 50 mL pentane, centrifuged, and the solution was decanted off and the residue was freeze-dried. All polymer samples were analyzed using NMR and SEC.

3.5. Activity Measurements

For measuring the activity of catalyst **4** towards 2VP and DEVP polymerization, 22.5 mg (22.5 μmol, 1.0 equiv.) of **4** were weighed into a screw cap vial and were dissolved in 10 mL dry toluene. Under vigorous stirring, the monomer (2VP: 400 equiv., DEVP: 600 equiv.) was added in one portion. At certain time intervals, 0.2 mL aliquots of the reaction mixture were taken out and quenched by addition of 0.4 mL wet methanol-d₄. The conversion of 2VP was determined from ¹H-NMR, while for DEVP, conversion was calculated from ³¹P-NMR. The aliquot NMRs were precipitated in 12 mL pentane, decanted off and dried in vacuo. The number-average molecular weight and polydispersity were determined using SEC (P2VP) or SEC-MALS (PDEVP). The turnover frequency was determined from the highest slope in the time-conversion plot and the normalized turnover frequency from an average initiator efficiency of these points. The living-type character of the polymerizations are determined from a linear increase of molecular weight in a conversion-molar mass plot.

3.6. Polymer Deprotection

(A) TBAF-deprotection: 150 mg PDEVP were dissolved in 10 mL dry tetrahydrofuran and 0.1 mmol of a 1 M TBAF solution in tetrahydrofuran was added. The reaction mixture was stirred for 24 h under ambient conditions. The solvent was removed in vacuo and the residue was subjected to dialysis in water (Spectra/Por 1 dialysis tubing, regenerated cellulose, molar-mass cut-off 5 kg mol⁻¹, 2 L water, five-fold solvent exchange). The residual polymer solution was dried and freeze-dried twice from high purity water.

(B) HCl-deprotection: 170 mg P2VP was dissolved in 6 mL ethanol and 0.6 mL concentrated HCl_(aq) were added. The reaction mixture was stirred for 24 h under ambient conditions and afterwards the solvent was removed in vacuo. The residue was dissolved in dichloromethane and an excess of concentrated sodium hydrogen carbonate solution was added to deprotonate the pyridine side chain protonation of the P2VP polymer. After phase separation, the aqueous phase was extracted with dichloromethane twice. The organic phases were combined, and the solvent was removed in vacuo prior to freeze-drying from 1,4-dioxane.

(C) AcOH-deprotection: The polymer (140 mg P2VP/250 mg PDEVP) was dissolved in 5 mL of a mixture of glacial acetic acid-tetrahydrofuran-water in a ratio of 3:1:1, and the mixture was stirred for 24 h. For P2VP, the work-up from reaction (B) was applied, while PDEVP was dissolved in dichloromethane after solvent removal and purified via precipitation in excess of pentane and followed by freeze-drying from 1,4-dioxane.

4. Conclusions

A novel silicon protected hydroxy-pyridine initiator was synthesized and used for functionalization of [(ONOO^tBuY(CH₂TMS)(thf)] via C–H bond activation to obtain a novel [(ONOO^tBuY(X)(thf)] (X = 4-(4'-(((tert-butylidimethylsilyl)oxy)methyl)phenyl)-2,6-di-methylpyridine) complex in high purity and yield. Activity measurements of this complex showed a high initiator efficiency in the REM-GTP of DEVP and 2VP and the living character of the polymerization was proven. A series of well-defined polymers with different molecular weights and small polydispersities were obtained. End-group characterization via mass spectrometry and 2D-NMR studies revealed a covalent attachment of the silicon protected initiator to the obtained polymers. A good agreement between the absolute number average molecular weights obtained via SEC and those calculated via NMR-spectra using the silyl end-group also proof a quantitative attachment. Different deprotection routes for the silyl-protection group were evaluated for all polymers and with the use of glacial acetic acid full deprotection was facilitated obtaining hydroxyl-terminated PDEVP and P2VP while maintaining full structural integrity of the polymers.

Supplementary Materials: The following are available online at <http://www.mdpi.com/2073-4344/10/4/448/s1>, Figure S1: ¹H-NMR (400 MHz, C₆D₆, 300 K) of catalyst 4; Figure S2: ¹³C-NMR (125 MHz, C₆D₆, 300 K) of catalyst 4; Figure S3: DOSY-NMR (CDCl₃, 400 MHz) of PDEVP ($M_n = 43.4 \text{ kg mol}^{-1}$, $D = 1.11$); Figure S4: DOSY-NMR (MeOD, 400 MHz) of P2VP ($M_n = 34.7 \text{ kg mol}^{-1}$, $D = 1.07$); Figure S5: ¹H-NMR (CDCl₃, 400 MHz) of PDEVP produced with catalyst 4 (Table 2, entry 4, $M_{n,\text{abs}} = 16.6 \text{ kg/mol}$, $D = 1.04$), impurities and artefacts are marked with *; Figure S6: ³¹P-NMR (CDCl₃, 162 MHz) of PDEVP produced with catalyst 4 (Table 2, entry 5, $M_{n,\text{abs}} = 104 \text{ kg/mol}$, $D = 1.33$); Figure S7: Representative SEC-MALS trace (top) and resulting fitting plot (bottom) for molecular weight determination of PDEVP produced with catalyst 4 (Table 2, entry 5, $M_{n,\text{abs}} = 104 \text{ kg/mol}$, $D = 1.33$); Figure S8: ¹H-NMR (CDCl₃, 400 MHz) of P2VP produced with catalyst 4 (Table 3, entry 1, $M_{n,\text{abs}} = 25.0 \text{ kg/mol}$, $D = 1.04$), impurities and artefacts are marked with *; Figure S9: ¹³C-NMR (MeOD, 500 MHz) of P2VP and section of the quaternary ¹³C atom resonance of atactic P2VP produced with catalyst 4, resonance assignment and microstructure determination according to ref. [1], impurities and artefacts are marked with *; Figure S10: Representative SEC-trace (top) and distribution plot of molecular weight determination (bottom) of P2VP produced with catalyst 4 (Table 2, entry 3, $M_{n,\text{abs}} = 22.6 \text{ kg/mol}$, $D = 1.06$). Signals in the light scattering detectors (orange, red) with retention time below 10 min are not detectable via RI (dark blue), therefore signals do not belong to polymeric material; Figure S11: Representative comparison of ¹H-NMR spectra of protected (bottom) and deprotected (top) P2VP (Table 4, entry 2) with close-up of the silyl region (TBDMS signals marked blue); Figure S12: Overlay of SEC RI traces of P2VP protected and deprotected (Table 4, entry 2) (protected black,

deprotected blue); Figure S13: Representative comparison of ^1H -NMRs of protected (bottom) and unprotected (top) PDEVP (Table 4, entry 1) with close-up of the silyl region (TBDMS signals marked blue); Figure S14: Overlay of SEC-MALS RI traces of PDEVP (Table 4, entry 1) protected and deprotected (protected black, deprotected blue, Synthesis procedures of **1** and **2**.

Author Contributions: Conceptualization, M.K., T.M.P. and F.A.; methodology, F.A. and A.S.; formal analysis, M.K. and T.M.P.; investigation, M.K. and T.M.P.; resources, B.R.; data curation, M.K., T.M.P. and F.A.; writing—original draft preparation, M.K.; writing—review and editing, T.M.P., F.A., A.S. and B.R.; visualization, M.K., F.A.; supervision, F.A. and B.R.; project administration, B.R.; funding acquisition, B.R. All authors have read and agree to the published version of the manuscript.

Funding: F.A. thanks the Bavarian State Ministry of Environment and Consumer Protection for financial support within BayBiotech research network. M.K. thanks the Studienstiftung des deutschen Volkes for their support via their PhD scholarship.

Acknowledgments: All authors want to acknowledge the team from elemental analysis by the Laboratory for Microanalytics at the Institute of Inorganic Chemistry at Technical University of Munich, Department of Chemistry, Catalysis Research Center.

Conflicts of Interest: The authors declare no conflict of interest.

References

1. Webster, O.W.; Hertler, W.R.; Sogah, D.Y.; Farnham, W.B.; RajanBabu, T.V. Group-transfer polymerization. 1. A new concept for addition polymerization with organosilicon initiators. *J. Am. Chem. Soc.* **1983**, *105*, 5706–5708. [[CrossRef](#)]
2. Yasuda, H.; Yamamoto, H.; Yokota, K.; Miyake, S.; Nakamura, A. Synthesis of monodispersed high molecular weight polymers and isolation of an organolanthanide(III) intermediate coordinated by a penultimate poly(MMA) unit. *J. Am. Chem. Soc.* **1992**, *114*, 4908–4910. [[CrossRef](#)]
3. Yasuda, H.; Ihara, E. Rare earth metal initiated polymerizations of polar and nonpolar monomers to give high molecular weight polymers with extremely narrow molecular weight distribution. *Macromol. Chem. Phys.* **1995**, *196*, 2417–2441. [[CrossRef](#)]
4. Yasuda, H.; Ihara, E.; Nitto, Y.; Kakehi, T.; Morimoto, M.; Nodono, M. Organo Rare Earth Metal Initiated Living Polymerizations of Polar and Nonpolar Monomers. In *Functional Polymers*; Patil, A.O., Schulz, D.N., Novak, B.M., Eds.; American Chemical Society: Washington, DC, USA, 1998; Volume 704, pp. 149–162.
5. Chen, E.Y.-X. Coordination polymerization of polar vinyl monomers by single-site metal catalysts. *Chem. Rev.* **2009**, *109*, 5157–5214. [[CrossRef](#)]
6. Salzinger, S.; Rieger, B. Rare Earth metal-mediated group transfer polymerization of vinylphosphonates. *Macromol. Rapid Commun.* **2012**, *33*, 1327–1345. [[CrossRef](#)] [[PubMed](#)]
7. Adams, F.; Pahl, P.; Rieger, B. Metal-Catalyzed Group-Transfer Polymerization: A Versatile Tool for Tailor-Made Functional (Co)Polymers. *Chem. Eur. J.* **2018**, *24*, 509–518. [[CrossRef](#)] [[PubMed](#)]
8. Collins, S.; Ward, D.G. Group-transfer polymerization using cationic zirconocene compounds. *J. Am. Chem. Soc.* **1992**, *114*, 5460–5462. [[CrossRef](#)]
9. Altenbuchner, P.T.; Adams, F.; Kronast, A.; Herdtweck, E.; Pöthig, A.; Rieger, B. Stereospecific catalytic precision polymerization of 2-vinylpyridine via rare earth metal-mediated group transfer polymerization with 2-methoxyethylamino-bis(phenolate)-yttrium complexes. *Polym. Chem.* **2015**, *6*, 6796–6801. [[CrossRef](#)]
10. Xu, T.-Q.; Yang, G.-W.; Lu, X.-B. Highly Isotactic and High-Molecular-Weight Poly(2-vinylpyridine) by Coordination Polymerization with Yttrium Bis(phenolate) Ether Catalysts. *ACS Catal.* **2016**, *6*, 4907–4913. [[CrossRef](#)]
11. Fuchise, K.; Chen, Y.; Satoh, T.; Kakuchi, T. Recent progress in organocatalytic group transfer polymerization. *Polym. Chem.* **2013**, *4*, 4278. [[CrossRef](#)]
12. Knaus, M.G.M.; Giuman, M.M.; Pöthig, A.; Rieger, B. End of Frustration: Catalytic Precision Polymerization with Highly Interacting Lewis Pairs. *J. Am. Chem. Soc.* **2016**, *138*, 7776–7781. [[CrossRef](#)]
13. Zhang, Y.; Miyake, G.M.; Chen, E.Y.-X. Alane-based classical and frustrated Lewis pairs in polymer synthesis: Rapid polymerization of MMA and naturally renewable methylene butyrolactones into high-molecular-weight polymers. *Angew. Chem. Int. Ed.* **2010**, *49*, 10158–10162. [[CrossRef](#)]

14. Salzinger, S.; Seemann, U.B.; Plikhta, A.; Rieger, B. Poly(vinylphosphonate)s Synthesized by Trivalent Cyclopentadienyl Lanthanide-Induced Group Transfer Polymerization. *Macromolecules* **2011**, *44*, 5920–5927. [[CrossRef](#)]
15. Soller, B.S.; Salzinger, S.; Rieger, B. Rare Earth Metal-Mediated Precision Polymerization of Vinylphosphonates and Conjugated Nitrogen-Containing Vinyl Monomers. *Chem. Rev.* **2016**, *116*, 1993–2022. [[CrossRef](#)]
16. Chen, X.; Caporaso, L.; Cavallo, L.; Chen, E.Y.-X. Stereoselectivity in metallocene-catalyzed coordination polymerization of renewable methylene butyrolactones: From stereo-random to stereo-perfect polymers. *J. Am. Chem. Soc.* **2012**, *134*, 7278–7281. [[CrossRef](#)]
17. Salzinger, S.; Soller, B.S.; Plikhta, A.; Seemann, U.B.; Herdtweck, E.; Rieger, B. Mechanistic studies on initiation and propagation of rare earth metal-mediated group-transfer polymerization of vinylphosphonates. *J. Am. Chem. Soc.* **2013**, *35*, 13030–13040. [[CrossRef](#)]
18. Soller, B.S.; Salzinger, S.; Jandl, C.; Pöthig, A.; Rieger, B. C–H Bond Activation by σ -Bond Metathesis as a Versatile Route toward Highly Efficient Initiators for the Catalytic Precision Polymerization of Polar Monomers. *Organometallics* **2014**, *34*, 2703–2706. [[CrossRef](#)]
19. Altenbuchner, P.T.; Soller, B.S.; Kissling, S.; Bachmann, T.; Kronast, A.; Vagin, S.I.; Rieger, B. Versatile 2-Methoxyethylaminobis(phenolate)yttrium Catalysts: Catalytic Precision Polymerization of Polar Monomers via Rare Earth Metal-Mediated Group Transfer Polymerization. *Macromolecules* **2014**, *47*, 7742–7749. [[CrossRef](#)]
20. Mariott, W.R.; Chen, E.Y.-X. Stereospecific, Coordination Polymerization of Acrylamides by Chiral ansa-Metallocenium Alkyl and Ester Enolate Cations. *Macromolecules* **2004**, *37*, 4741–4743. [[CrossRef](#)]
21. Rodriguez-Delgado, A.; Mariott, W.R.; Chen, E.Y.-X. Living and Syndioselective Polymerization of Methacrylates by Constrained Geometry Titanium Alkyl and Enolate Complexes. *Macromolecules* **2004**, *37*, 3092–3100. [[CrossRef](#)]
22. Weger, M.; Grötsch, R.K.; Knaus, M.G.; Giuman, M.M.; Mayer, D.C.; Altmann, P.J.; Mossou, E.; Dittrich, B.; Pöthig, A.; Rieger, B. Non-Innocent Methylene Linker in Bridged Lewis Pair Initiators. *Angew. Chem. Int. Ed.* **2019**, *58*, 9797–9801. [[CrossRef](#)] [[PubMed](#)]
23. Weger, M.; Giuman, M.M.; Knaus, M.G.; Ackermann, M.; Drees, M.; Hornung, J.; Altmann, P.J.; Fischer, R.A.; Rieger, B. Single-Site, Organometallic Aluminum Catalysts for the Precise Group Transfer Polymerization of Michael-Type Monomers. *Chem. Eur. J.* **2018**, *24*, 14950–14957. [[CrossRef](#)] [[PubMed](#)]
24. Weger, M.; Pahl, P.; Schmidt, F.; Soller, B.S.; Altmann, P.J.; Pöthig, A.; Gemmecker, G.; Eisenreich, W.; Rieger, B. Isospecific Group-Transfer Polymerization of Diethyl Vinylphosphonate and Multidimensional NMR Analysis of the Polymer Microstructure. *Macromolecules* **2019**, *52*, 7073–7080. [[CrossRef](#)]
25. Zhang, N.; Salzinger, S.; Soller, B.S.; Rieger, B. Rare earth metal-mediated group-transfer polymerization: From defined polymer microstructures to high-precision nano-scaled objects. *J. Am. Chem. Soc.* **2013**, *135*, 8810–8813. [[CrossRef](#)]
26. Miyake, G.M.; Chen, E.Y.-X. Metallocene-Mediated Asymmetric Coordination Polymerization of Polar Vinyl Monomers to Optically Active, Stereoregular Polymers. *Macromolecules* **2008**, *41*, 3405–3416. [[CrossRef](#)]
27. Kaneko, H.; Nagae, H.; Tsurugi, H.; Mashima, K. End-functionalized polymerization of 2-vinylpyridine through initial C–H bond activation of N-heteroaromatics and internal alkynes by yttrium ene-diamido complexes. *J. Am. Chem. Soc.* **2011**, *133*, 19626–19629. [[CrossRef](#)]
28. Adams, F.; Machat, M.R.; Altenbuchner, P.T.; Ehrmaier, J.; Pöthig, A.; Karsili, T.N.V.; Rieger, B. Toolbox of Nonmetallocene Lanthanides: Multifunctional Catalysts in Group-Transfer Polymerization. *Inorg. Chem.* **2017**, *56*, 9754–9764. [[CrossRef](#)]
29. Adams, F.; Altenbuchner, P.T.; Werz, P.D.L.; Rieger, B. Multiresponsive micellar block copolymers from 2-vinylpyridine and dialkylvinylphosphonates with a tunable lower critical solution temperature. *RSC Adv.* **2016**, *6*, 78750–78754. [[CrossRef](#)]
30. Adams, F.; Pschenitza, M.; Rieger, B. Yttrium-Catalyzed Synthesis of Bipyridine-Functionalized AB-Block Copolymers: Micellar Support for Photocatalytic Active Rhenium-Complexes. *ChemCatChem* **2018**, *10*, 4309–4316. [[CrossRef](#)]
31. Schwarzenböck, C.; Schaffer, A.; Nößner, E.; Nelson, P.J.; Huss, R.; Rieger, B. Fluorescent Polyvinylphosphonate Bioconjugates for Selective Cellular Delivery. *Chem. Eur. J.* **2018**, *24*, 2584–2587. [[CrossRef](#)]

32. Schwarzenböck, C.; Schaffer, A.; Pahl, P.; Nelson, P.J.; Huss, R.; Rieger, B. Precise synthesis of thermoresponsive polyvinylphosphonate-biomolecule conjugates via thiol–ene click chemistry. *Polym. Chem.* **2018**, *9*, 284–290. [[CrossRef](#)]
33. Altenbuchner, P.T.; Werz, P.D.L.; Schöppner, P.; Adams, F.; Kronast, A.; Schwarzenböck, C.; Pöthig, A.; Jandl, C.; Haslbeck, M.; Rieger, B. Next Generation Multiresponsive Nanocarriers for Targeted Drug Delivery to Cancer Cells. *Chem. Eur. J.* **2016**, *22*, 14576–14584. [[CrossRef](#)] [[PubMed](#)]
34. Pahl, P.; Schwarzenböck, C.; Herz, F.A.D.; Soller, B.S.; Jandl, C.; Rieger, B. Core-First Synthesis of Three-Armed Star-Shaped Polymers by Rare Earth Metal-Mediated Group Transfer Polymerization. *Macromolecules* **2017**, *50*, 6569–6576. [[CrossRef](#)]
35. Arndtsen, B.A.; Bergman, R.G.; Mobley, T.A.; Peterson, T.H. Selective Intermolecular Carbon-Hydrogen Bond Activation by Synthetic Metal Complexes in Homogeneous Solution. *Acc. Chem. Res.* **2002**, *28*, 154–162. [[CrossRef](#)]
36. Labinger, J.A.; Bercaw, J.E. Understanding and exploiting C–H bond activation. *Nature* **2002**, *417*, 507–514. [[CrossRef](#)]
37. Goldberg, K.I.; Goldman, A.S. (Eds.) *Activation and Functionalization of C—H Bonds*; American Chemical Society: Washington, DC, USA, 2004.
38. Adams, F.; Rieger, B. From Michael-Type Systems to Biobased Lactones: Designing Novel Polymer Microstructures with Modified Bis(phenolate)lanthanides. Ph.D. Thesis, Technical University Munich, Munich, Germany, 2019. Available online: <http://nbn-resolving.de/urn/resolver.pl?urn:nbn:de:bvb:91-diss-20190123-1464556-1-9> (accessed on 1 April 2020).
39. Watson, P.L. Facile C–H activation by lutetium–methyl and lutetium–hydride complexes. *J. Chem. Soc. Chem. Commun.* **1983**, 276–277. [[CrossRef](#)]
40. Watson, P.L. Methane exchange reactions of lanthanide and early-transition-metal methyl complexes. *J. Am. Chem. Soc.* **1983**, *105*, 6491–6493. [[CrossRef](#)]
41. Schaffer, A.; Kränlein, M.; Rieger, B. Synthesis and Application of Functional Group-Bearing Pyridyl-based Initiators to Rare-Earth Metal-Mediated Group-Transfer Polymerization. *Macromolecules*. under review.
42. Zhang, N.; Salzinger, S.; Deubel, F.; Jordan, R.; Rieger, B. Surface-initiated group transfer polymerization mediated by rare earth metal catalysts. *J. Am. Chem. Soc.* **2012**, *134*, 7333–7336. [[CrossRef](#)]
43. Ajellal, N.; Carpentier, J.-F.; Guillaume, C.; Guillaume, S.M.; Helou, M.; Poirier, V.; Sarazin, Y.; Trifonov, A.A. Bridging the gap in catalysis via multidisciplinary approaches. *Dalton Trans.* **2010**, *39*, 8354.
44. Anastasaki, A.; Nikolaou, V.; Nurumbetov, G.; Wilson, P.; Kempe, K.; Quinn, J.F.; Davis, T.P.; Whittaker, M.R.; Haddleton, D.M. Cu(0)-Mediated Living Radical Polymerization: A Versatile Tool for Materials Synthesis. *Chem. Rev.* **2016**, *116*, 835–877. [[CrossRef](#)]
45. Matyjaszewski, K. Advanced Materials by Atom Transfer Radical Polymerization. *Adv. Mater.* **2018**, *30*, e1706441. [[CrossRef](#)] [[PubMed](#)]
46. Bonnet, M.; Hong, C.R.; Wong, W.W.; Liew, L.P.; Shome, A.; Wang, J.; Gu, Y.; Stevenson, R.J.; Qi, W.; Anderson, R.F.; et al. Next-Generation Hypoxic Cell Radiosensitizers: Nitroimidazole Alkylsulfonamides. *J. Med. Chem.* **2018**, *61*, 1241–1254. [[CrossRef](#)] [[PubMed](#)]
47. Doundoulakis, T.; Xiang, A.X.; Lira, R.; Agrios, K.A.; Webber, S.E.; Sisson, W.; Aust, R.M.; Shah, A.M.; Showalter, R.E.; Appleman, J.R.; et al. Myxopyronin B analogs as inhibitors of RNA polymerase, synthesis and biological evaluation. *Bioorg. Med. Chem. Lett.* **2004**, *14*, 5667–5672. [[CrossRef](#)] [[PubMed](#)]
48. Greene, T.W.; Wuts, P.G.M. *Protective Groups in Organic Synthesis*, 3rd ed.; Wiley-Interscience: Hoboken, NJ, USA, 2002; pp. 201–270.
49. Nelson, T.D.; Crouch, R.D. Selective Deprotection of Silyl Ethers. *Synthesis* **1996**, *1996*, 1031–1069. [[CrossRef](#)]
50. Seemann, U.B. Polyvinylphosphonate und Deren Copolymere Durch Seltenerdmetall Initiierte Gruppen-Transfer-Polymerisation. Ph.D. Thesis, Technical University Munich, Munich, Germany, 2010. Available online: <http://nbn-resolving.de/urn/resolver.pl?urn:nbn:de:bvb:91-diss-20101013-992998-1-7> (accessed on 1 April 2020).

51. Tshuva, E.Y.; Groysman, S.; Goldberg, I.; Kol, M.; Goldschmidt, Z. [ONXO]-Type Amine Bis(phenolate) Zirconium and Hafnium Complexes as Extremely Active 1-Hexene Polymerization Catalysts. *Organometallics* **2002**, *21*, 662–670. [[CrossRef](#)]
52. Hultzsch, K.C.; Voth, P.; Beckerle, K.; Spaniol, T.P.; Okuda, J. Single-Component Polymerization Catalysts for Ethylene and Styrene: Synthesis, Characterization, and Reactivity of Alkyl and Hydrido Yttrium Complexes Containing a Linked Amido–Cyclopentadienyl Ligand. *Organometallics* **2000**, *19*, 228–243. [[CrossRef](#)]



© 2020 by the authors. Licensee MDPI, Basel, Switzerland. This article is an open access article distributed under the terms and conditions of the Creative Commons Attribution (CC BY) license (<http://creativecommons.org/licenses/by/4.0/>).